BCSJ

Stereochemical Stability Differences between Axially Chiral 6-Aryl-Substituted Picolinic Esters and Their Benzoic Ester Derivatives: sp^2N: vs. sp^2CH in CH_3, C_6H_5, and CH_3O ortho-Substitution Effect

Shinji Tanaka,[3] Yusuke Suzuki,[1] Masaharu Matsushita,[2] and Masato Kitamura*[1]

[1]Graduate School of Pharmaceutical Sciences, Nagoya University, Chikusa-ku, Nagoya, Aichi 464-8601

[2]Graduate School of Science, Nagoya University, Chikusa-ku, Nagoya, Aichi 464-8601

[3]Research Center for Materials Science, Nagoya University, Chikusa-ku, Nagoya, Aichi 464-8601

E-mail: kitamura@os.rcms.nagoya-u.ac.jp

Received: July 30, 2015; Accepted: September 4, 2015; Web Released: December 15, 2015

Masato Kitamura

Masato Kitamura received his Doctor of Agriculture at Nagoya University (NU) (Professors T. Goto and M. Isobe) in 1983. After postdoctoral work with Professor G. Stork (Columbia University), he joined the Noyori group at Faculty of Science in NU as Assistant Professor (1983), and was promoted to Associate Professor (1990). In 1998, he moved to Research Center for Materials Science in NU as Full Professor. Currently, he is studying at Graduate School of Pharmaceutical Sciences in NU from 2012. He is a recipient of The CSJ Award for Young Chemists (1989) and Synthetic Organic Chemistry Award, Japan (2012).

Abstract

An axially chiral naphthyl-substituted picolinic acid (R-Naph-PyCOOH) or its allyl ester (R-Naph-PyCOOAll) acts as an excellent ligand for catalytic asymmetric dehydrative intramolecular allylation. Towards the future development of a high performance catalysis using R-Naph-PyCOOH or its carba-analogue (R-Naph-PhCOOH), the stereochemical stability of R-Naph-PyCOOAll and R-Naph-PhCOOAll has been investigated by a systematic change in the ortho-substituent R on the naphthalene ring from CH_3 to C_6H_5 and CH_3O to provide a range of effective radius (ER) and Hammett standard σ constant (σ_p). Enantiomerically pure R-Naph-PyCOOAll and R-Naph-PhCOOAll were prepared, and the rotational energy barriers $\Delta G^{\ddagger}(sp^2N)$ and $\Delta G^{\ddagger}(sp^2CH)$ as well as the racemization half-life ($t_{1/2}$) were determined by time-interval chiral HPLC analysis of the enantiomer ratio (er). These experiments revealed have been i) that replacement of sp^2CH with sp^2N lowers $\Delta G^{\ddagger}$ at least by 14 kJ mol^{-1} (3.3 kcal mol^{-1}), and ii) that the degree of the $\Delta G^{\ddagger}$ lowering ($\Delta\Delta G^{\ddagger}$) is not proportional to ER, but has a high linear correlation to σ_p with a negative ρ value. In this particular system, a synergistic effect of the steric and electronic factors stabilizes $TS_{\phi 180}$ with a 180° dihedral angle of $CH_3OC(2')=C(1')-C(6)=N(1)$ over $TS_{\phi 0}$, decreasing the $t_{1/2}$ of CH_3O-Naph-PyCOOAll to 7 days from 1600 years of CH_3-Naph-PyCOOAll.

Axially chiral biaryls have constituted one of the core structural motifs in chiral ligands,[1] molecular machines,[2] and both natural and unnatural biologically active compounds[3] since the atropisomerism of 6,6′-dinitro-2,2′-diphenic acid was first detected in 1922.[4] The stereochemical stability of individual enantiomers is determined mainly by the steric factor of the ortho-substituents of the biphenyls (Ph-Ph), ***L***, ***S***, ***L′***, and ***S′***, where ***L*** and ***L′*** are larger in size than ***S*** and ***S′***, respectively (Figure 1a), and is generally discussed by use of the concept of the effective radius (ER), as defined by Sternhell.[5] Replacement of sp^2C–***S*** with sp^2N reduces the rotational energy barrier $\Delta G^{\ddagger}$ value because the ***S*** substituent then is replaced by the lone pair on N (Figure 1b). In 2009, Clayden quantitatively investigated the substituent effect in the rotation through the sp^2C–sp^2C bond joining two aryl rings in 6-phenylpyridine derivatives (Ph-Py) by use of a dynamic NMR technique (DNMR).[6] Two years later, Schlosser estimated the degree of space-filling of a pyridine lone pair in

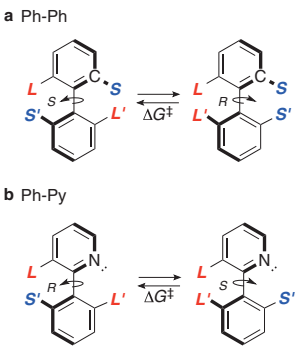

Figure 1. Atropisomerism of ortho-substituted biaryl compounds Ph-Ph and Ph-Py (***L*** > ***S***; ***L′*** > ***S′***). The upper aryl ring is fixed for simplicity.

comparison to the corresponding C–H analogue by DNMR and a DFT calculation of systematically designed Ph-Py and Ph-Ph compounds, and revealed that the $\Delta G^{\ddagger}$ values of Ph-Pys are up to 17.6 kJ mol^{-1} (4.2 kcal mol^{-1}) smaller than those of the carba-analogous Ph-Phs.[7] Thanks to these pioneering studies, the torsional barriers of Ph-Pys can now be discussed as an extension of those of Ph-Ph-derivatives, enabling the rational design and synthesis of various axially chiral Ph-Py-type ligands in asymmetric catalysts.[1c,1d]

We have recently found that axially chiral (*S*)- or (*R*)-Cl-Naph-PyCOOAll ((*S*)- or (*R*)-allyl 6-(2-chloronaphthalen-1-yl)-5-methylpyridine-2-carboxylic ester) (**1**) works as an excellent ligand in combination with [RuCp(CH$_3$CN)$_3$]PF$_6$ for catalytic asymmetric dehydrative cyclization of various allylic alcohols having protonic nucleophiles, as shown in Figure 2.[8] Their use enables efficient enantioselective construction of hetero- and carbo-cycles, which are key chiral starting materials for the synthesis of pharmaceuticals and natural products. This first example of the high utility of chiral picolinic acid derivatives, as well as the first successful example of a paradigm shift from traditional salt-liberation-type Tsuji–Trost allylation to the H_2O-liberation version, attracted a great deal of attention from the organic synthetic chemist community.[8e,8f] Here, we would like to report the results of a quantitative analysis of the stereochemical stability of a series of new axially chiral ligands as a step towards the design of chiral picolinic acid derivatives and carba-analogues with a much higher performance in asymmetric catalysis.

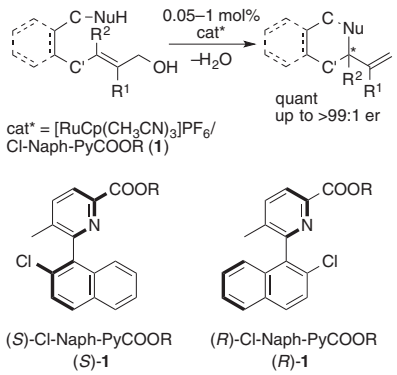

Figure 2. Asymmetric dehydrative cyclization of ω-NuH-substituted allylic alcohols (NuH: OH, NHCOR, NHSO$_2$R, COOH) catalyzed by a CpRu(II) complex with a new axially chiral picolinic acid-type ligand. R = H or CH$_2$CH=CH$_2$ (All).

Results and Discussion

System Design. Figure 3 represents the general energy diagram for the racemization of ortho-disubstituted biaryls (X = sp^{2}N and sp^{2}CH). As defined in Figure 1, ***L*** and ***L′*** are larger substituents than ***S***, which is either H or a lone pair in this particular case, and ***S′***, respectively. The conformation in the ground state is expected to be orthogonal because both aryl rings have ortho-substituted skeletons. Clockwise rotation of the lower aryl ring through the sp^{2}C–sp^{2}C single bond gives a planar transition state TS$_{\phi 0}$. Here, s-cis ***S′***–C=C–C=X with the dihedral angle of 0° generates a relatively less crowded cove region, while the two large ortho-substituents, ***L*** and ***L′***, on the same side creates an over crowded fjord region.[9] Anticlockwise rotation gives TS$_{\phi 180}$, in which small sp^{2}N: or sp^{2}CH and large ***L′*** are located in the cove region and ***L*** and ***S′*** are in the fjord region. The ***S***/***L′*** (H or lone pair/***L′***) and ***L***/***S′*** combination is preferred over the ***S***/***S′*** (H or lone pair/***S′***) and ***L***/***L′*** combination, and therefore the enantiomer more easily inverts the stereochemistry via TS$_{\phi 180}$. At first glance, the ER size of ***L*** and ***S′*** might be thought to be the decisive factor determining the $\Delta G^{\ddagger}$ value of TS$_{\phi 180}$, but the actual situation is not so simple. The TS could be stabilized or destabilized by electronic factors involving a conjugation in ***S′***–C=C–C=X or ***L′***–C=C–C=X and an electronic repulsion between ***S′*** or ***L′*** and sp^{2}N. In order to avoid complications in analysis of the steric and electronic effects on the stereochemical stability of future axially chiral ligands, the basic skeletons are fixed to be allyl 5-methyl-6-(2-R-naphthyl)picolinate (**2**, R-Naph-PyCOOAll) and the benzoate analogues (**3**, R-Naph-PhCOOAll) (Chart 1), in which three R groups, CH$_3$ (ER, 1.80 Å; σ_p, −0.14), C$_6$H$_5$ (1.62, 0.02), and CH$_3$O (1.52, −0.28), are adopted. The carboxylic acid was protected as the allyl (All) ester to avoid protonation of the sp^{2}N atom.

Synthesis of (±)-R-Naph-PyCOOAll and (±)-R-Naph-PhCOOAll. For the purposes of this quantitative study of rotation around the C(6)–C(1′) bond of the sp^{2}N-type chiral **2**

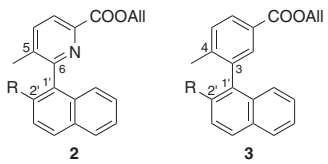

Chart 1.

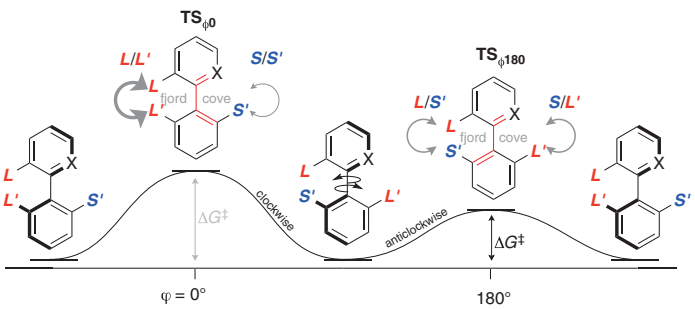

Figure 3. Schematic energy diagram in the racemization process of ortho-disubstituted biaryls (X = sp^{2}N and sp^{2}CH). ***L*** > X (***S***), ***L′*** > ***S′*** > X (***S***). The upper aryl ring is fixed for simplicity.

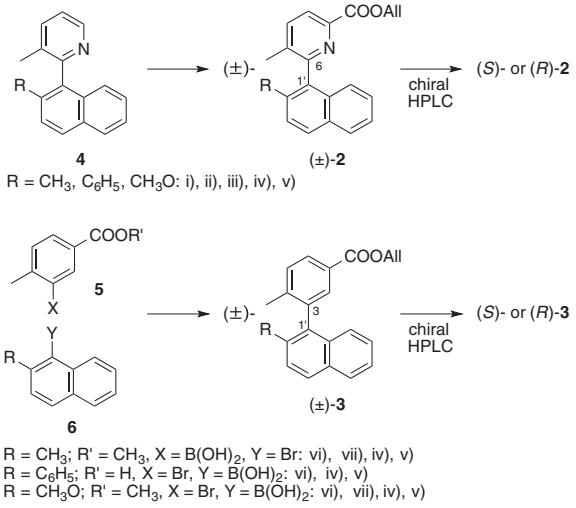

Figure 4. Systematic synthesis of (±)-R-Naph-PyCOOAll ((±)-**2**) and (±)-R-Naph-PhCOOAll ((±)-**3**). i) mCPBA. ii) $ClCON(CH_3)_2$, $(CH_3)_3SiCN$. iii) aq HCl. iv) $SOCl_2$. v) AllOH. vi) $[Pd(P(C_6H_5)_3)_4]$, Na_2CO_3 or K_2CO_3. vii) aq NaOH. Chiral HPLC separation: CHIRALCEL OD-H for **2a**, **2b**, and **3c**; CHIRALPAK AD-H for **2c**, **3a**, and **3b**.

and C(3)–C(1′) bond for the sp^2CH-type chiral **3**, six racemic compounds were initially prepared in a systematic way as shown in Figure 4. The reaction conditions were not optimized. All of the precursors, **4a** (R = CH_3),[8a] **4b** (R = C_6H_5),[8a] and **4c** (R = CH_3O),[10] for the **2** series are known compounds. These were converted in 32–61% overall yields in 5 steps via i) N-oxidation, ii) Reissert–Henze cyanation, iii) acid-promoted hydrolysis, iv) acid chloride formation, and v) alcoholysis by AllOH. The corresponding carba-analogues **3** were also similarly synthesized in 36–78% overall yields from benzoic acid derivatives **5** (X = $B(OH)_2$, R′ = CH_3 for **3a**; X = Br, R′ = H for **3b**; X = Br, R′ = CH_3 for **3c**) via i) Suzuki–Miyaura coupling with **6** (Y = Br for **3a**, Y = $B(OH)_2$ for **3b** and **3c**), ii) acid chloride formation, and iii) alcoholysis by AllOH. With **5** (R′ = CH_3), a hydrolysis step is required after the C(3)–C(1′) coupling.

Enantiomer Separation. The *R* and *S* enantiomers of (±)-**2** and (±)-**3** were separated by use of a preparative HPLC packed with a chiral stationary phase (**2a**, **2b**, and **3c**: CHIRALCEL OD-H; **2c**, **3a**, and **3b**: CHIRALPAK AD-H) by 10 injections, each being 2 mg (Figure 4). The absolute configurations of the longer retention time **2a** and **2b** compounds were determined to be *R* and *S*, respectively, by the X-ray crystallographic analyses of (1*R*,2*S*,5*R*)-menthyl ester of CH_3-Naph-PyCOOH and (*R*)-1-phenylethylamide of C_6H_5-Naph-PyCOOH. The details are described in the previous report.[8a] As there was no correlation between the HPLC elution order and the configuration in the above two cases, the absolute configurations of **2c**, **3a**, **3b**, and **3c** were not assigned.

Racemization. The enantiomerically pure **2a**–**2c** and **3a**–**3c** obtained above were used for measurement of the racemization rate constants k_{rac}. The standard conditions were set to [**2** or **3**] = 10 mM, DMA, and 120 °C (393 K). At appropriate time intervals, an aliquot of the mixture was sampled and subjected to chiral HPLC analysis to determine the enantiomer ratio (er). Figure 5a(1) shows the change in the er of **2a** over time. The er decreases from >99:1 to 85:15 (11 h), 77:23 (20 h), 66:34 (38 h), and 54:46 (81 h). Logarithmic plots of the enantiomeric excess (ee = $|R - S|/|R + S|$), converted from the er values, versus time is shown in Figure 5a(2). The linear relationship, $\ln(ee) = -8.64 \times 10^{-6}t + 4.61$, with a correlation coefficient (R^2) of 0.998 determined the k_{rac} value to be $8.64 \times 10^{-6}\,s^{-1}$. The energy barrier $\Delta G^{\ddagger}$ for the *R*/*S* stereoinversion can be empirically related to $8.314T\ln(2.084 \times 10^{10}\,T/k_{rac})$ by use of the Eyring equation,[11] therefore $\Delta G^{\ddagger}$ at 120 °C was calculated to be 135 kJ mol^{-1} (33 kcal mol^{-1}). The half-life ($t_{1/2}$) of (*R*)-**2a** was deduced from $\ln 2/k_{rac}$ to be 1600 years at 25 °C. Figures 5b–5f shows the HPLC profiles as well as the exponential decay curves for **2b**, **2c**, **3a**, **3b**, and **3c**. Since the decline in the er of **2c** was too fast to measure under the standard conditions,[6i] the rate of racemization was measured at 50 °C. Table 1 summarizes the results together with the effective radius (ER) and Hammett standard σ_p constant for R as indices for the steric effect and the electronic effect, respectively.

Effect of Substituent R on Stereochemical Stability. As expected from Schlosser's investigation,[7] the rotation energy barrier $\Delta G^{\ddagger}$(CH) values of sp^2CH-type biaryls **3** are higher than the $\Delta G^{\ddagger}$(N) values of sp^2N-type biaryl **2** in all cases with R = CH_3, C_6H_5, and CH_3O (Table 1). Among the six compounds **2a**–**2c** and **3a**–**3c**, **3a** is stereochemically the most stable with a barrier of 153 kJ mol^{-1} (36.3 kcal mol^{-1}) and 1500000 years half life, while **2c** is the most unstable, where the $\Delta G^{\ddagger}$ and $t_{1/2}$ values decrease to 107 kJ mol^{-1} (25.6 kcal mol^{-1}) and 7 days, respectively. The significant difference in the stereochemical stability is apparently ascribable to the following two steric factors: i) sp^2N (lone pair) vs. sp^2CH (H) in the upper aryl ring and ii) CH_3 (1.80 ER) and CH_3O (1.52 ER) at C(2′) of the lower naphthalene ring. The smaller substituent combination in **2c** remarkably facilitates the C(6)–C(1′) bond rotation, while the larger substituent combination in **3a** impedes the C(3)–C(1′) bond rotation. Interestingly, however, the energy difference $\Delta\Delta G^{\ddagger}$ between $\Delta G^{\ddagger}$(CH) and $\Delta G^{\ddagger}$(N) is not proportional to the ER value: 18 kJ mol^{-1} (4.3 kcal mol^{-1}) for R = CH_3 (1.80 ER); 14 kJ mol^{-1} (3.3 kcal mol^{-1}) for R = C_6H_5 (1.62 ER); 23 kJ mol^{-1} (5.5 kcal mol^{-1}) for R = CH_3O (1.52 ER). A correlation can be seen rather between $\Delta\Delta G^{\ddagger}$ and the Hammett standard σ constant, σ_p, for R. As the σ_p value decreases from 0.02 to −0.14 and −0.28, the $\Delta\Delta G^{\ddagger}$ value increases from 14 to 18 and then 23, implying that there is an electronic effect in the sp^2N-type R-Naph-PyCOOAll that does not exist in the sp^2CH analogue R-Naph-PhCOOAll. As shown in Figure 6, the Hammett plot of $\Delta\Delta G^{\ddagger}$ versus σ_p exhibited a linear relationship with a correlation coefficient of 0.99. Although there are only three data points, the high linear correlation with a negative slope ($\rho = -29.9$) clearly indicates that the degree of decrease in the TS energy level produced by the replacement of sp^2CH with sp^2N increases as the electron donor character of R increases.

In the present biaryls, R-Naph-PyCOOAll and R-Naph-PhCOOAll, the sp^2C–sp^2C bond rotation is thought to proceed via $TS_{\phi 180}$, as in the general discussion in Figure 3. With R = CH_3O, however, the s-trans conformation is preferred over the corresponding s-cis conformation of $TS_{\phi 0}$ for both steric and electronic reasons (Figure 7a). The ***L***/***S***′ combination (***L***:

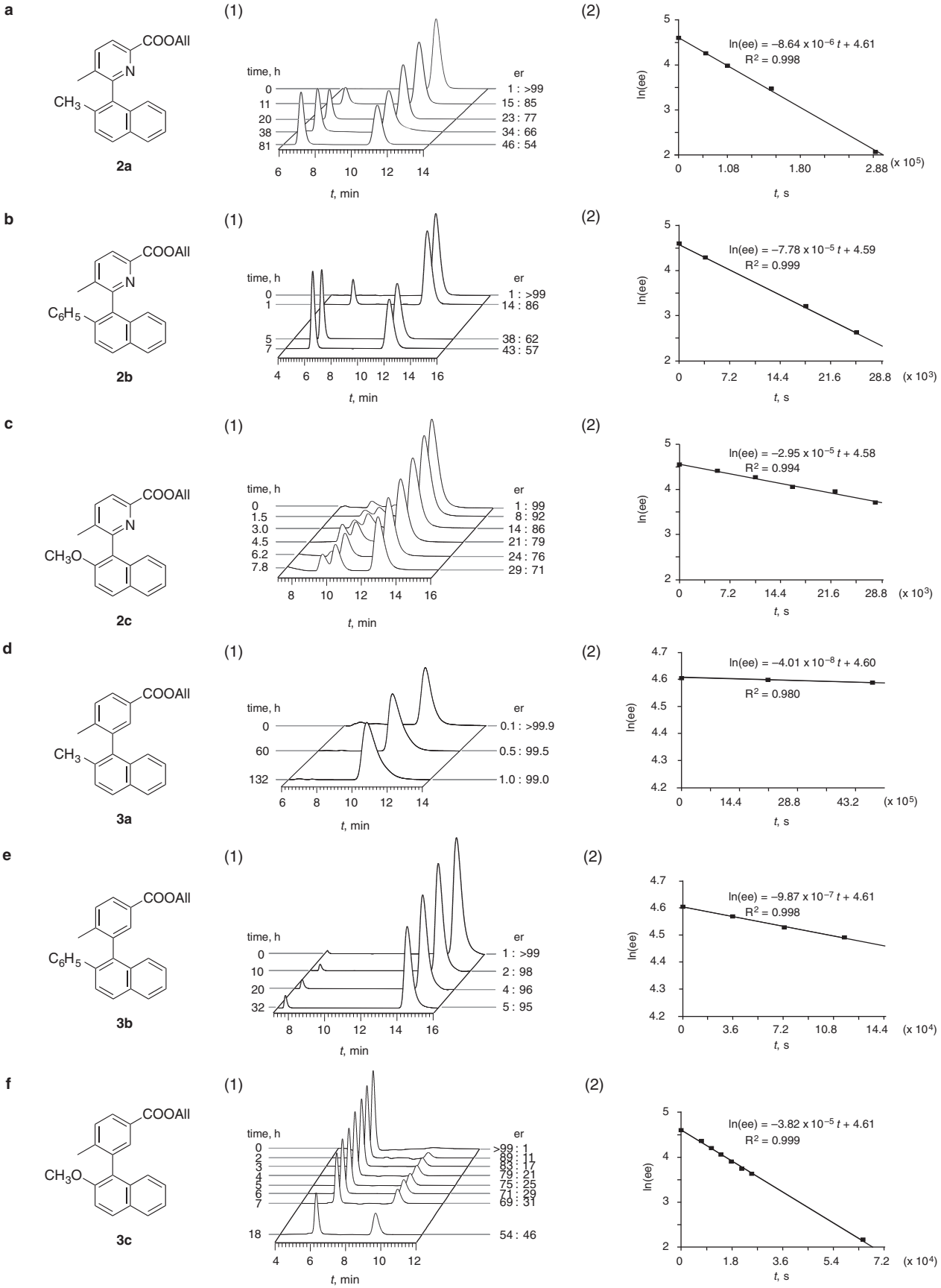

Figure 5. Determination of the racemization rate k_{rac}, the rotational energy barrier $\Delta G^{\ddagger}$, and the half-life $t_{1/2}$. (1): HPLC charts of **2** and **3** sampled at appropriate time intervals. (2): the logarithmic plots of the ees over time.

Table 1. Relation between effective radius (ER) and Hammett standard σ constant (σ_p) for R and the rotational energy barrier $\Delta G^{\ddagger}$ for the enantiomerically pure R-Naph-PyCOOAll and R-Naph-PhCOOAll (R = CH_3, C_6H_5, and CH_3O)[a)]

Entry	R	**2**		**3**		$\Delta\Delta G^{\ddagger}$	ER/Å	σ_p
		$\Delta G^{\ddagger}_{393K}$/kJ mol^{-1} [c)]	$t_{1/2\cdot 298K}$	$\Delta G^{\ddagger}_{393K}$/kJ mol^{-1} [c)]	$t_{1/2\cdot 298K}$			
1	CH_3	135	1600 y	153	1500000 y	18	1.80	−0.14
2	C_6H_5	128	100 y	142	27000 y	14	1.62	0.02
3	CH_3O	107[b)]	7 d	130	200 y	23	1.52	−0.28

a) Conditions: [**2** or **3**] = 10 mM; DMA; 120 °C. b) 50 °C (323 K). c) Calculated by the Eyring equation.

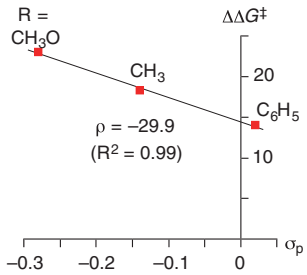

Figure 6. Hammett plots of $\Delta\Delta G^{\ddagger}$ as a function of σ_p values.

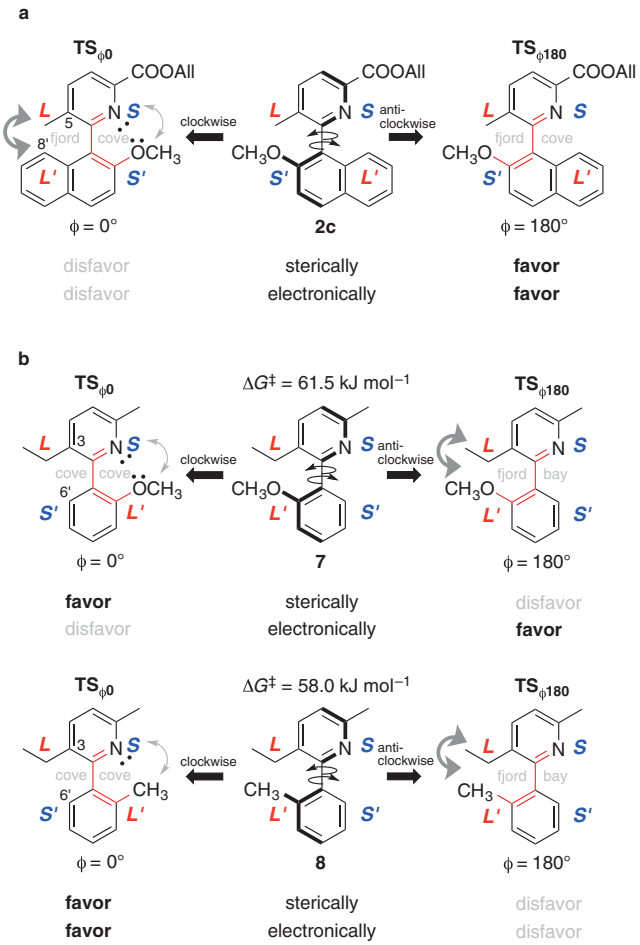

Figure 7. Supposed transient planar structures of CH_3O-Naph-PyCOOAll (**2c**) and the related aryl-pyridine compounds **7** and **8**.

$C(5)CH_3$, ***S′***: CH_3O) in the fjord region is sterically less disfavored than the ***L***/***L′*** combination (***L***: $C(5)CH_3$, ***L′***: C(8′)H). The degree of conjugation in the CH_3O–C=C–C=N moiety is enhanced by the involvement of an n-orbital on the O of the CH_3O substituent, and the dipole moment generated by the anti-located C=N and CH_3O–C decreases the molecular polarity. This synergistic effect would be a reason for the easier racemization of **2c** in comparison to **2a** and **2b**. On the contrary, the situation is completely reversed by alteration of the 2-naphthalenepyridine systems **2** to 2-phenylpyridine systems **7** and **8** (Figure 7b). The rotation barrier of **7** (R = CH_3O) is 3.5 kJ mol^{-1} (0.8 kcal mol^{-1}) higher than that of **8** (R = CH_3) (61.5 kJ mol^{-1} (14.7 kcal mol^{-1}) vs. 58.0 kJ mol^{-1} (13.9 kcal mol^{-1})) as reported by Clayden.[6a] The tendency is consistent neither with the ER-based view, nor with our observations. As shown in Figure 3, the anticlockwise/clockwise route to $TS_{\phi 180}$ or $TS_{\phi 0}$ is determined by the relative ER-size difference between the ortho-substituents on the two aryl rings. The ***S***/***L′***–***L***/***S′*** combination is sterically advantageous in comparison to the ***S***/***S′***–***L***/***L′*** combination. In the case of **7** (R = CH_3O), as shown in Figure 7b, the clockwise rotation gives a sterically favored, but electronically disfavored, $TS_{\phi 0}$ (***S***/***L′***–***L***/***S′***: sp^2N:/CH_3O–C(3)Et/C(6′)H), and the anticlockwise rotation has sterically disfavored, but electronically favored, $TS_{\phi 180}$ (***S***/***S′***–***L***/***L′***: sp^2N:/C(6′)H–C(3)Et/CH_3O). The higher $\Delta G^{\ddagger}$ value of **7** (R = CH_3O, 1.52 ER) than that of **8** (R = CH_3, 1.80 ER) might indicate a racemization process that proceeds via $TS_{\phi 0}$. Electronic repulsion caused between the sp^2N lone pair and CH_3O lone pairs would raise the rotational energy more than expected simply from their ER values.

Conclusion

Information on the stereochemical stability of axially chiral compounds serves as a platform for designing chiral functional materials, particularly chiral ligands that can contribute to the development of catalytic asymmetric reactions. Taking advantage of our groundbreaking finding of the utility of a chiral picolinic acid-type ligand in a Ru-catalyzed asymmetric dehydrative allylation,[8] the stereochemical stability of enantiomerically pure R-Naph-PyCOOAll (**2**) and the carba-analogue R-Naph-PhCOOAll (**3**) have been investigated in a systematic way by fixing R at C(2′) of the naphthalene ring to CH_3 (1.80 ER; −0.14 σ_p), C_6H_5 (1.62 ER; 0.02 σ_p), and CH_3O (1.52 ER; −0.28 σ_p), and by setting the upper aryl group to allyl 5-methylpicolinate or allyl 4-methylbenzoate. The steric and electronic effect of R on the rotational energy barrier $\Delta G^{\ddagger}$ as well as the racemization half-life $t_{1/2}$ was quantitatively analyzed to reveal i) that the replacement of sp^2C(2)H in **3** with sp^2N lowers $\Delta G^{\ddagger}$ at least by 14 kJ mol^{-1} (3.3 kcal mol^{-1}), and

ii) that the degree of the $\Delta G^{\ddagger}$ lowering ($\Delta\Delta G^{\ddagger}$) is not proportional to ER, but has a high linear correlation to σ_p with a negative ρ value in the Hammett plot. The phenomenon could be understood by a synergistic effect of the steric and electronic factors. With the particular biaryl **2**, $TS_{\phi 180}$ with the s-trans-CH_3O–C(2′)=C(1′)–C(6)=N(1) is both sterically and electronically preferred over $TS_{\phi 0}$, decreasing the $t_{1/2}$ of **2c** (R = CH_3O) to 7 days from the 1600 years of the methyl derivative **2a** (R = CH_3). In contrast, R-Ph-Py-type biaryls **7** and **8** show a reversed pattern, in which the $\Delta G^{\ddagger}$ value of **7** (R = CH_3O) is 6% higher than that of **8** (R = CH_3). A mismatch between the steric and electronic factors for the stabilization of the TS causes the reversed effect. One tends to recognize the sp^2N only as a smaller substituent for sp^2CH, but these results show that care must be taken when designing a pyridine-containing axially chiral biaryl ligand, particularly in an electronically conjugatable system.

Experimentals

Instruments. Nuclear magnetic resonance (NMR) spectra were recorded on a JEOL JNM-ECA-600 (600 MHz for ^1H, and 152 MHz for ^{13}C), and the chemical shifts are expressed in parts per million (ppm) downfield from $Si(CH_3)_4$ or in ppm relative to $CHCl_3$ (δ 7.26) in ^1H NMR and to $CDCl_3$ (δ 77.0) in ^{13}C NMR. The ^1H signal coupling patterns are indicated as follows: s, singlet; d, doublet; t, triplet; q, quartet; m, multiplet; and br, broad signal. The resolutions of the ^1H- and ^{13}C NMR spectra were 0.689 and 1.44 Hz, respectively. All of the NMR spectra were measured at 25 °C. High-resolution mass spectra (HRMS) were measured by ESI on a Bruker Daltonics micrOTOF-QII system. A Shimadzu 10AD with 6A pump was used for high performance liquid chromatography (HPLC) analyses as well as preparative separation of enantiomers.

Materials. Gas: Argon (Ar) gas was purified by being passed through a column of BASF R3-11 catalyst at 80 °C and then through a column of granular $CaSO_4$.

Solvents: Solvents for preparation of ligands and for the racemization experiments were dried and degassed at the reflux temperature in the presence of appropriate drying agents (2.5 g L^{-1}) under an Ar stream for 6 h and then distilled into the storage part of the distillation system: tetrahydrofuran (THF) and 1,2-dimethoxyethane (DME) from sodium benzophenone ketyl; dichloromethane (CH_2Cl_2) and *N*,*N*-dimethylacetaminde (DMA) from CaH_2. The CH_2Cl_2 used for the distillation was first distilled over P_2O_5, and kept in the presence of molecular sieves 4A (MS 4A). Chloroform-*d* ($CDCl_3$) was purchased from Cambridge Isotope Laboratories, and passed through ICN-Alumina-B-Super I (5 g/100 mL) before use. HPLC grade ethyl acetate (EtOAc), hexane, and 2-propanol (*i*-PrOH) were used for analysis of enantiomer ratios (er) and for separation of enantiomers using the chiral HPLC column. First grade CH_2Cl_2, diethyl ether (Et_2O), and hexane were used for extraction and flash silica-gel column chromatography (SiO_2-chromatography) without purification: Distilled water (H_2O) was used for reactions, and tap water for extraction.

Reagents and Chemicals. All reagents were purchased from companies and used without further purification. These are listed below in the alphabetical order neglecting the number suffix. Aldrich: 1,2-dibromoethane ($(BrCH_2)_2$) and (2-methoxynaphthalen-1-yl)boronic acid. Kishida chemical: allyl alcohol (AllOH), sodium bicarbonate ($NaHCO_3$), sodium hydroxide (NaOH), and sodium sulfonate (Na_2SO_4). Nacalai Tesque: distilled water (distilled H_2O), 12 M hydrochloric acid H_2O solution (12 M aqueous HCl), potassium carbonate (K_2CO_3), sodium carbonate (Na_2CO_3), thionyl chloride ($SOCl_2$), and magnesium (Mg). Tokyo Chemical Industry: 3-bromo-4-methylbenzoic acid, 1-bromo-2-methylnaphthalene, triethyl borate ($(EtO)_3B$), methyl 3-bromo-4-methylbenzoate, *N*,*N*-dimethylcarbamoyl chloride ($ClCONMe_2$), trimethylsilyl cyanide (TMSCN), and tetrakis(triphenylphosphine)palladium(0) ($[Pd(PPh_3)_4]$). Wako: 69–75% *m*-chloroperoxybenzoic acid (mCPBA) and sodium chloride (NaCl). The following compounds for the synthesis of **2c**, **3a**, **3b**, and **3c** were prepared in accordance with reported procedures: 2-(2-methoxynaphthalen-1-yl)-3-methylpyridine,[9] [5-(methoxycarbonyl)-2-methylphenyl]boronic acid,[12] 1-bromo-2-phenylnaphthalene.[13]

General Manipulations. A Teflon-coated magnetic bar was used for stirring a reaction mixture. Reactions at 0 °C and at −78 °C were carried out by use of an ice bath and of a dry ice/CH_3OH bath, respectively. Room temperature (rt) was in the range of 25 to 28 °C. Remaining solvents after a general workup process were removed by means of a rotary evaporator. Concentration of a reaction mixture in a Schlenk flask was performed by connecting to a vacuum-Ar line via a cold trap cooled by liquid N_2. Organic extracts obtained by a general partition-based workup were dried over anhydrous Na_2SO_4 for ca. 30 min. "Aqueous" and "saturated" are abbreviated as "aq" and "sat," respectively. Brine means sat aq NaCl. All of organometallic reactions were carried out under an Ar atmosphere using a general Schlenk technique unless otherwise specified. A Schlenk flask with a Teflon J. Young valve is specified as a "Young-type Schlenk." Schlenk flasks were dried before use at ca. 250 °C by use of a heat gun under a reduced pressure, and silicon grease was used for connecting to a cold finger and a glass stopper. Liquid reagents were introduced by use of a syringe via a septum rubber. After introduction, the septum was replaced with a glass stopper or with a Young valve. Heating in a closed system was carried out after reducing the pressure of the whole system or after raising the temperature, followed by closing the system. A cold finger was used for reflux processes in the Schlenk system. Solvents and liquid chemicals were transferred by use of a gas-tight syringe or cannulation method. One freeze-thaw cycle consists of i) freezing a liquid mixture, ii) evacuation of the system at the freezing stage, iii) closing the system, iv) thawing the frozen liquid, and v) releasing the negative pressure to atmospheric pressure by filling with Ar gas. The reaction conditions for the synthesis of ligands were not optimized.

Synthesis of (±)-R-Naph-PyCOOAll and (±)-R-Naph-PhCOOAll. (±)-CH_3-Naph-PyCOOAll ((±)-**2a**) and (±)-C_6H_5-Naph-PyCOOAll ((±)-**2b**) were prepared in accordance with reported procedures.[8a]

(±)-CH_3O-Naph-PyCOOAll ((±)-2c). The procedures essentially followed those reported in ref 8a.

Process I: A 50-mL Schlenk flask was charged with 2-(2-methoxynaphthalen-1-yl)-3-methylpyridine (1.17 g, 4.68 mmol)[9] and CH_2Cl_2 (10 mL). The resulting colorless solution was cooled to 0 °C, and three portions of mCPBA (69–75%,

1.62 g) were added at 10-min intervals. The temperature was gradually raised to rt, and the colorless solution was stirred for 30 min. After cooling again to 0 °C, 1 M aq NaOH (10 mL) was slowly added. The organic layer was washed with 1 M aq NaOH (10 mL) and brine (10 mL), and then dried over Na_2SO_4 (5 g). Filtration/evaporation gave 2-(2-methoxynaphthalen-1-yl)-3-methylpyridine-1-oxide as a brownish oil (986 mg), which was immediately used for Process ii without further purification.

Process II: A 100-mL Schlenk flask was charged with the above obtained crude *N*-oxide compound (986 mg) and CH_2Cl_2 (30.0 mL). To the brown solution was added $ClCONMe_2$ (560 mg, 5.20 mmol) dissolved in CH_2Cl_2 (10.0 mL). After 30 min at rt, TMSCN (738 mg, 7.44 mmol) dissolved in CH_2Cl_2 (10.0 mL) was added. The Schlenk line was equipped with a cold finger. The whole mixture was stirred at rt for 12 h, and then heated at 50 °C for 3 h. After cooling down to rt, the mixture was washed with sat aq $NaHCO_3$ (20 mL) and H_2O (20 mL), and the organic layer was separated and concentrated to give 6-(2-methoxynaphthalen-1-yl)-5-methylpicolinonitrile as a brown oil (1.5 g), which was immediately used for Process iii without further purification.

Process III: The crude nitrile compound (1.5 g) and 6 M aq HCl (10.0 mL) were placed in a 50-mL round-bottomed flask equipped with a reflux condenser. The whole mixture was heated at 100 °C for 12 h, cooled to rt and concentrated in vacuo. To this crude residue containing 6-(2-methoxynaphthalen-1-yl)-5-methylpicolinic acid was added $SOCl_2$ (5.00 mL), and the mixture was stirred at rt for 2 h. Removal of all of the volatiles in vacuo gave a crude acid chloride as a brown oil, which was dissolved in CH_2Cl_2 (4.00 mL) and AllOH (1.50 mL). After 2 h at rt, the mixture was concentrated in vacuo. The residue was dissolved in CH_2Cl_2 (20 mL). This was washed with sat aq $NaHCO_3$ (10 mL × 2), and dried over Na_2SO_4 (ca. 5 g). Filtration/evaporation afforded a brown solid, which was purified by SiO_2-chromatography (50 g, 1:8 EtOAc–hexane eluent) to give (±)-**2a** as a white solid (500 mg, 32% total yield): ^{1}H NMR ($CDCl_3$): δ 2.09 (s, 3H, CH_3), 3.83 (s, 3H, OCH_3), 4.85–4.92 (m, 2H, $COOCH_2CHCH_2$), 5.26 (dd, J = 10.33, 1.38 Hz, 1H, $COOCH_2CHCHH$), 5.39 (dd, J = 17.21, 1.38 Hz, 1H, $COOCH_2CHCHH$), 6.01–6.07 (m, 1H, $COOCH_2CHCH_2$), 7.09 (dd, J = 8.26, 1.38 Hz, 1H, aromatic proton (ar)), 7.29–7.35 (m, 3H, ar), 7.78 (d, J = 7.57 Hz, 1H, ar), 7.81 (dd, J = 7.23, 2.07 Hz, 1H, ar), 7.92 (d, J = 8.95 Hz, 1H, ar); ^{13}C NMR ($CDCl_3$): δ 19.2, 56.7, 66.3, 113.5, 118.7, 122.7, 123.8, 124.3, 124.5, 126.9, 128.1, 129.4, 130.4, 132.4, 133.2, 138.2, 138.5, 146.0, 154.3, 156.7, 165.5; HRMS m/z ($M + Na^+$) obsd 356.1277, calcd for $C_{21}H_{19}NNaO_3$ 356.1257.

(±)-CH_3-Naph-PhCOOAll ((±)-3a). Process I: A 20-mL Schlenk flask was charged with [5-(methoxycarbonyl)-2-methylphenyl]boronic acid (200 mg, 1.03 mmol),[12] 1-bromo-2-methylnaphthalene (80.0 µL, 521 µmol), 2.00 M aq Na_2CO_3 (1.00 mL, 2.00 mmol), and DME (4.00 mL). After degassing the whole mixture by three freeze-thaw cycles, to the suspension was added [$Pd(PPh_3)_4$] (60.0 mg, 51.9 µmol). The mixture was heated at 100 °C for 18 h. The reaction mixture was cooled to rt, and then the diphase solution was acidified by addition of 1 M aq HCl (10 mL). This was extracted with CH_2Cl_2 (10 mL × 3), and the organic extracts were dried over Na_2SO_4 (ca. 5 g), filtered, and concentrated to give the crude product (0.3 g) as a yellow oil. This was used for the next reaction without further purification.

Process II: To the yellow oil compound (0.3 g) charged into a 50 mL round-bottom flask was added dioxane (5.00 mL), H_2O (5.00 mL), and NaOH (120 mg, 3.00 mmol). After being stirred at rt for 18 h, the reaction mixture was acidified by addition of 1 M aq HCl (3 mL), and then the aq layer was extracted with EtOAc (10 mL × 4). The combined organic layers were washed with brine (30 mL), and dried over Na_2SO_4 (ca. 10 g). Filtration/evaporation afforded a white solid (249 mg), which was used for the next reaction without further purification.

Process III: To the white solid product (249 mg) placed in a 20-mL Schlenk flask was added $SOCl_2$ (3.00 mL), and the mixture was stirred at 60 °C for 2 h. After removal of the volatiles in vacuo, AllOH (3.00 mL) was added at rt. The mixture was stirred at rt for 6 h, and concentrated in vacuo to give a yellow oil (ca. 0.5 g). The residue was purified by SiO_2-chromatography (50 g, 1:20 EtOAc–hexane eluent) to give (±)-allyl 4-methyl-3-(2-methylnaphthalen-1-yl)benzoate ((±)-**3a**) as a white solid (254 mg, 78% total yield): ^{1}H NMR ($CDCl_3$): δ 1.98 (s, 3H, CH_3), 2.15 (s, 3H, CH_3), 4.80 (d, J = 5.50 Hz, 2H, $COOCH_2CHCH_2$), 5.25 (d, J = 11.0 Hz, 1H, $COOCH_2CHCHH$), 5.38 (d, J = 17.2 Hz, 1H, $COOCH_2CHCHH$), 6.01 (m, 1H, $COOCH_2CHCH_2$), 7.16 (d, J = 8.25 Hz, ar), 7.31 (dd, J = 7.56, 7.56 Hz, 1H, ar), 7.40–7.45 (m, 3H, ar), 7.81 (d, J = 8.25 Hz, 1H, ar), 7.84 (s, 1H, ar), 7.85 (d, J = 9.62 Hz, 1H, ar), 8.06 (dd, J = 9.62, 1.37 Hz, 1H, ar); ^{13}C NMR ($CDCl_3$): δ 19.8, 20.3, 65.5, 118.3, 124.9, 125.4, 126.1, 127.5, 127.9, 128.2, 128.6, 128.8, 130.2, 131.3, 132.0, 132.3, 133.2, 136.3, 139.5, 142.8, 166.4; HRMS m/z ($M + Na^+$) obsd 339.1357, calcd for $C_{22}H_{20}NaO_2$ 339.1356.

(±)-C_6H_5-Naph-PhCOOAll ((±)-3b). Process I: A 50-mL three-necked round-bottomed flask equipped with a dropping funnel, a reflux condenser, and a three-way stopcock was charged with Mg (45.7 mg, 1.88 mmol), THF (10.0 mL), and two drops of $(BrCH_2)_2$. A 10-mL THF solution of 1-bromo-2-phenylnaphthalene (443 mg, 1.56 mmol)[13] was introduced for 1 h from a dropping funnel so as to keep a gentle reflux. After another 1-h stirring followed by cooling to −78 °C, $(EtO)_3B$ (0.530 mL, 3.13 mmol) was added, and the temperature was raised to rt. The mixture was stirred at rt for 5 h, and partitioned between 2 M aq HCl (10 mL) and Et_2O (15 mL). The aq layer was extracted with Et_2O (15 mL × 3), and the combined extracts were washed with brine (15 mL). Drying over Na_2SO_4 (ca. 10 g)/filtration/evaporation afforded a crude product containing ca. 50% of (2-phenylnaphtalene-1-yl)boronic acid, which was used for the next process without further purification.

Process II: The procedure was the same as Process I in the synthesis of (±)-**3a**. Conditions: the above obtained crude (2-phenylnaphthalene-1-yl)boronic acid (424 mg, 0.782 mmol as the pure form); 3-bromo-4-methylbenzoic acid (368 mg, 1.71 mmol), 2 M aq K_2CO_3 (2.28 mL); DME (4.60 mL); [$Pd(PPh_3)_4$] (93.0 mg, 80.5 µmol); 100 °C; 12 h. The crude product (1.16 g) was used for Process iii without purification.

Process III: The procedure was the same as Process II in the synthesis of (±)-**3a**. Conditions: the above obtained crude

4-methyl-3-(2-phenylnaphthalen-1-yl)benzoic acid (1.16 g); $SOCl_2$ (5.00 mL); AllOH (5.00 mL). Purification: 2-times SiO_2-chromatography (1st, 100 g, 1:6 EtOAc–hexane eluent; 2nd, 50 g, 1:6 EtOAc–hexane eluent). (±)-Allyl 4-methyl-3-(2-phenylnaphthalen-1-yl)benzoate ((±)-**3b**) (90.0 mg, 36% total yield): ^{1}H NMR ($CDCl_3$): δ 1.89 (s, 3H, CH_3), 4.76–4.79 (m, 2H, $COOCH_2CHCH_2$), 5.25 (dd, $J = 11.02$, 1.38 Hz, 1H, $COOCH_2CHCHH$), 5.35 (dd, $J = 17.21$, 1.38 Hz, 1H, $COOCH_2CHCHH$), 5.70–6.03 (m, 1H, $COOCH_2CHCH_2$), 7.15–7.18 (m, 5H, ar), 7.28 (d, $J = 8.26$ Hz, 1H, ar), 7.34 (d, $J = 8.26$ Hz, 1H, ar), 7.39 (ddd, $J = 8.66$, 8.57, 1.38 Hz, 1H, ar), 7.50 (ddd, $J = 7.57$, 7.57, 1.38 Hz, 1H, ar), 7.59 (d, $J = 8.26$ Hz, 1H, ar), 7.90–7.97 (m, 4H, ar); ^{13}C NMR ($CDCl_3$): δ 19.8, 20.3, 65.5, 118.3, 124.9, 125.4, 126.1, 127.5, 127.9, 128.2, 128.6, 128.8, 130.2, 131.3, 132.0, 132.3, 133.2, 136.3, 139.5, 142.8, 166.4; HRMS m/z ($M + Na^+$) obsd 401.1523, calcd for $C_{27}H_{22}NaO_2$ 401.1512.

(±)-CH_3O-Naph-PhCOOAll ((±)-3c). The procedures were the same as Processes I–III in the synthesis of (±)-**3a**.

Process I: Conditions: (2-methoxynaphthalen-1-yl)boronic acid (300 mg, 1.49 mmol); methyl 3-bromo-4-methylbenzoate (136 µL, 873 µmol); 2 M aq Na_2CO_3 (1.75 mL, 3.50 mmol); DME (5.00 mL); $[Pd(PPh_3)_4]$ (101 mg, 87.4 µmol); 100 °C; 18 h. The crude product (0.5 g) was directly used for the next reaction.

Process II: Conditions: dioxane (5.00 mL); H_2O (5.00 mL); NaOH (86.2 mg, 2.15 mmol); rt, 16 h. The crude product (0.2 g) was used for the next allylation.

Process III: Conditions: the above obtained crude 3-(2-methoxynaphthalen-1-yl)-4-methylbenzoic acid (0.2 g); $SOCl_2$ (3.00 mL); 60 °C; 2 h; AllOH (3.00 mL). Purification: SiO_2-chromatography (50 g, 1:15 EtOAc–hexane eluent). (±)-Allyl 3-(2-methoxynaphthalen-1-yl)-4-methylbenzoate (198 mg, 68% total yield): ^{1}H NMR ($CDCl_3$): δ 2.06 (s, 3H, CH_3), 3.84 (s, 3H, CH_3O), 4.80 (d, $J = 5.50$ Hz, 2H, $COOCH_2CHCH_2$), 5.25 (dd, $J = 10.3$, 1.37 Hz, 1H, $COOCH_2CHCHH$), 5.38 (dd, $J = 17.9$, 1.37 Hz, 1H, $COOCH_2CHCHH$), 5.98–6.04 (m, 1H, $COOCH_2CHCH_2$), 7.20 (d, $J = 8.25$ Hz, ar), 7.31–7.36 (m, 1H, ar), 7.38 (d, $J = 9.12$ Hz, 1H, ar), 7.44 (d, $J = 8.25$ Hz, 1H, ar), 7.84 (dd, $J = 8.26$, 1.38 Hz, 1H, ar), 7.90–7.93 (m, 2H, ar), 8.05 (dd, $J = 9.28$, 2.11 Hz, 1H, ar); ^{13}C NMR ($CDCl_3$): δ 20.0, 56.5, 65.4, 113.3, 118.1, 123.2, 123.6, 124.7, 126.6, 127.8, 128.0, 128.8, 129.0, 129.4, 130.0, 132.2, 132.4, 133.2, 136.5, 143.7, 153.7, 166.4; HRMS m/z ($M + Na^+$) obsd 339.1357, calcd for $C_{22}H_{20}NaO_2$ 339.1356.

Enantiomer Separation. Enantiomers of (±)-CH_3-Naph-PyCOOAll ((±)-**2a**) and (±)-C_6H_5-Naph-PyCOOAll ((±)-**2b**) were obtained in accordance with the procedures reported earlier.[8a] All other enantiomers were separated by chiral HPLC column under the following conditions, and were immediately subjected to the er decay experiments.

(±)-CH_3O-Naph-PyCOOAll ((±)-2c): Column, CHIRALPAK AD-H (2 cm $\phi \times 25$ cm); eluent, 9:1 hexane–*i*-PrOH; flow rate, 10 mL min^{-1}; detection, 254-nm light; t_R, 15.9 and 20.0 min; sample loading, 2 mg/injection × 10.

(±)-CH_3-Naph-PhCOOAll ((±)-3a): Column, CHIRALPAK AD-H (2 cm $\phi \times 25$ cm); eluent, 50:1 hexane–*i*-PrOH; flow rate, 10 mL min^{-1}; detection, 254-nm light; t_R, 15.45 and 18.67 min; sample loading, 2 mg/injection × 10.

(±)-C_6H_5-Naph-PhCOOAll ((±)-3b): Column, CHIRALPAK AD-H (2 cm $\phi \times 25$ cm); eluent, 10:1 hexane–*i*-PrOH; flow rate, 10 mL min^{-1}; detection, 254-nm light; t_R, 9.07 and 22.08 min; sample loading, 2 mg/injection × 10.

(±)-CH_3O-Naph-PhCOOAll ((±)-3c): Column, CHIRALCEL OD-H (2 cm $\phi \times 25$ cm); eluent, 5:1 hexane–*i*-PrOH; flow rate, 10 mL min^{-1}; detection, 254-nm light; t_R, 10.55 and 16.62 min; sample loading, 2 mg/injection × 10.

Determination of the Rotational Energy Barrier $\Delta G^{\ddagger}$ and $t_{1/2}$. A typical procedure is represented by that for the enantiomerically pure CH_3-Naph-PyCOOAll (**2a**). A 20-mL Young-type Schlenk flask was charged with **2a** (3.30 mg, 10.0 µmol) and DMA (1.00 mL). After degassing the system by three-freeze/thaw cycles, the mixture was heated at 120 °C by use of a Riko MH-5D oil bath, which was adjusted so that the measurement temperature was kept the same throughout the whole process. After 11 h, the Schlenk flask was moved to an ice bath, and an aliquot of the mixture (0.1 mL) was sampled under Ar. Immediately after sampling (5 min), the Schlenk flask was inserted into the 120 °C oil bath. The sample was partitioned between Et_2O (1 mL) and H_2O (1 mL). The organic layer was washed with H_2O (1 mL × 2), and concentrated in vacuo. This was subjected to er analysis by HPLC (column, CHIRALCEL OD-H (0.46 cm $\phi \times 25$ cm); eluent, 5:1 hexane–*i*-PrOH; flow rate, 1 mL min^{-1}; detection, 254-nm light; t_R, 7.22 and 11.43 min), determining the er to be 85.0:15.0. In the same way, the ers were measured at 20 h, 38 h, and 81 h to be 77.0:23.0, 66.25:33.75, and 54.0:46.0, respectively. The logarithmic plot of ln(ee) versus time determined the racemization rate k_{rac} to be 8.64×10^{-6} s^{-1}. By use of the Eyring equation ($\Delta G^{\ddagger} = 8.314T\ln(2.084 \times 10^{10}\, T/k_{rac})$), the rotational energy barrier $\Delta G^{\ddagger}$ was found to be 135.2 kJ mol^{-1} at 393 K. The HPLC charts and ln(ee)/time relation is shown in Figures 5a(1) and 5a(2), respectively. The HPLC conditions, ee change, k_{rac}, and $\Delta G^{\ddagger}$ values obtained for **2b**, **2c**, **3a**, **3b**, and **3c** are listed below. The er decay of **2c** was measured at 50 °C because of the stereochemical lability.

C_6H_5-Naph-PyCOOAll (2b): HPLC conditions: column, CHIRALCEL OD-H (0.46 cm $\phi \times 25$ cm); eluent, 85:15 hexane–*i*-PrOH; flow rate, 1 mL min^{-1}; detection, 254-nm light; t_R, 6.60 and 12.39 min. Ee change: 0 h (>99.9% ee), 1.0 h (72.6% ee), 5.0 h (25.1% ee), 7.0 h (13.6% ee). $k_{rac} = 7.78 \times 10^{-5}$ s^{-1}. $\Delta G^{\ddagger}_{393K} = 128.1$ kJ mol^{-1} (Figure 5b).

CH_3O-Naph-PyCOOAll (2c): HPLC conditions: column, CHIRALPAK AD-H (0.46 cm $\phi \times 25$ cm); eluent, 9:1 hexane–*i*-PrOH; flow rate, 1 mL min^{-1}; detection, 254-nm light; t_R, 10.50 and 12.98 min. The origin of the peak at 9.6 min is unidentified. Ee change: 0 h (97.4% ee), 1.5 h (84.4% ee), 3.0 h (72.0% ee), 4.5 h (58.5% ee), 6.2 h (52.8% ee), 7.8 h (42.0% ee) at 50 °C. $k_{rac} = 2.95 \times 10^{-5}$ s^{-1}. $\Delta G^{\ddagger}_{323K} = 107.3$ kJ mol^{-1} (Figure 5c).

CH_3-Naph-PhCOOAll (3a): HPLC conditions: column, CHIRALPAK AD-H (0.46 cm $\phi \times 25$ cm); eluent, 10:1 hexane–*i*-PrOH; flow rate, 1 mL min^{-1}; detection, 254-nm light; t_R, 7.71 and 10.41 min. Ee change: 0 h (>99.9% ee), 60 h (98.9% ee), 132 h (98.1% ee). $k_{rac} = 4.01 \times 10^{-8}$ s^{-1}. $\Delta G^{\ddagger}_{393K} = 152.8$ kJ mol^{-1} (Figure 5d).

C_6H_5-Naph-PhCOOAll (3b): HPLC conditions: column, CHIRALPAK AD-H (0.46 cm $\phi \times 25$ cm); eluent, 10:1 hex-

ane–*i*-PrOH; flow rate, 1 mL min^{-1}; detection, 254-nm light; t_R, 7.82 and 14.57 min. Ee change: 0 h (>99.9% ee), 10 h (96.4% ee), 20 h (92.7% ee), 32 h (89.3% ee). $k_{rac} = 9.87 \times 10^{-7}$ s^{-1}. $\Delta G^{\ddagger}_{393K} = 142.3$ kJ mol^{-1} (Figure 5e).

CH_3O-Naph-PhCOOAll (3c): HPLC conditions: column, CHIRALPAK AD-H (0.46 cm $\phi \times$ 25 cm); eluent, 10:1 hexane–*i*-PrOH; flow rate, 1 mL min^{-1}; detection, 254-nm light; t_R, 6.35 and 9.71 min. Ee change: 0 h (>99.9% ee), 2.0 h (78.6% ee), 3.0 h (66.9% ee), 4.0 h (58.1% ee), 5.0 h (50.0% ee), 6.0 h (42.3% ee), 7.0 h (37.6% ee), 18 h (8.68% ee). $k_{rac} = 3.82 \times 10^{-5}$ s^{-1}. $\Delta G^{\ddagger}_{393K} = 130.4$ kJ mol^{-1} (Figure 5f).

This work was aided by a Grant-in-Aid for Scientific Research (No. 25E07B212) and (Nos. 22750088, 24510112, and 24106713) from the Ministry of Education, Culture, Sports, Science and Technology (Japan), and an Advanced Catalytic Transformation Program for Carbon Utilization (ACT-C) from Japan Science and Technology Agency (JST).

Supporting Information

NMR spectra of **2c** and **3a**–**3c** and HPLC charts of **2c** and **3a**–**3c** for enantiomer separation. This material is available electronically on J-STAGE.

References

1 a) R. Noyori, H. Takaya, *Acc. Chem. Res.* **1990**, *23*, 345. b) Y. Chen, S. Yekta, A. K. Yudin, *Chem. Rev.* **2003**, *103*, 3155. c) J. M. Brunel, *Chem. Rev.* **2005**, *105*, 857. d) M. Berthod, G. Mignani, G. Woodward, M. Lemaire, *Chem. Rev.* **2005**, *105*, 1801. For the stereo controlled synthesis of axially and planary chiral compounds, see: e) K. Igawa, N. Ichikawa, Y. Ano, K. Katanoda, M. Ito, T. Akiyama, K. Tomooka, *J. Am. Chem. Soc.* **2015**, *137*, 7294. f) K. Tanaka, *Chem.—Asian J.* **2009**, *4*, 508. g) T. Kawabata, S. Kawakami, S. Majumdar, *J. Am. Chem. Soc.* **2003**, *125*, 13012. h) Y. Uozumi, T. Hayashi, *J. Am. Chem. Soc.* **1991**, *113*, 9887.

2 Review: W. R. Browne, B. L. Feringa, *Nat. Nanotechnol.* **2006**, *1*, 25.

3 a) C. Wolf, *Dynamic Stereochemistry of Chiral Compounds Principles and Applications*, RSC Publishing, **2008**. doi:10.1039/9781847558091. b) G. Bringmann, T. Gulder, T. A. M. Gulder, M. Breuning, *Chem. Rev.* **2011**, *111*, 563.

4 G. H. Christie, J. Kenner, *J. Chem. Soc., Trans.* **1922**, *121*, 614.

5 G. Bott, L. D. Field, S. Sternhell, *J. Am. Chem. Soc.* **1980**, *102*, 5618.

6 a) J. Clayden, S. P. Fletcher, J. J. W. McDouall, S. J. M. Rowbottom, *J. Am. Chem. Soc.* **2009**, *131*, 5331. For other reports on determination of stereochemical stability of 2-aryl-substituted pyridine, see: b) J. R. Pedersen, *Acta Chem. Scand.* **1972**, *26*, 929. c) S. C. Tucker, J. M. Brown, J. Oakes, D. Thornthwaite, *Tetrahedron* **2001**, *57*, 2545. d) F. Y. Kwong, Q. Yang, T. C. W. Mak, A. S. C. Chan, K. S. Chan, *J. Org. Chem.* **2002**, *67*, 2769. e) S. B. Cortright, R. A. Yoder, J. N. Johnston, *Heterocycles* **2004**, *62*, 223. f) R. W. Baker, S. O. Rea, M. V. Sargent, E. M. C. Schenkelaars, T. S. Tjahjandarie, A. Totaro, *Tetrahedron* **2005**, *61*, 3733. g) B. A. Sweetman, H. Müller-Bunz, P. J. Guiry, *Tetrahedron Lett.* **2005**, *46*, 4643. h) R. W. Baker, S. O. Rea, M. V. Sargent, E. M. C. Schenkelaars, T. S. Tjahjandarie, A. Totaro, *Tetrahedron* **2005**, *61*, 3733. i) M. Hapke, K. Kral, C. Fischer, A. Spannenberg, A. Gutnov, D. Redkin, B. Heller, *J. Org. Chem.* **2010**, *75*, 3993.

7 A. Mazzanti, L. Lunazzi, S. Lepri, R. Ruzziconi, M. Schlosser, *Eur. J. Org. Chem.* **2011**, 6725.

8 a) S. Tanaka, T. Seki, M. Kitamura, *Angew. Chem., Int. Ed.* **2009**, *48*, 8948. b) T. Seki, S. Tanaka, M. Kitamura, *Org. Lett.* **2012**, *14*, 608. c) Y. Suzuki, T. Seki, S. Tanaka, M. Kitamura, *J. Am. Chem. Soc.* **2015**, *137*, 9539. d) K. Miyata, M. Kitamura, *Synthesis* **2012**, *44*, 2138. e) M. Kitamura, K. Miyata, T. Seki, N. Vatmurge, S. Tanaka, *Pure Appl. Chem.* **2013**, *85*, 1121. f) M. Kitamura, S. Tanaka, M. Yoshimura, *J. Synth. Org. Chem., Jpn.* **2015**, *73*, 690.

9 J. C. Fetzer, *Large (C ≥ 24) Polycyclic Aromatic Hydrocarbons*, John Wiley & Sons, New York, **2000**.

10 A. Ros, B. Estepa, P. Ramírez-López, E. Álvarez, R. Fernández, J. M. Lassaletta, *J. Am. Chem. Soc.* **2013**, *135*, 15730.

11 For a report on determination of $\Delta G^{\ddagger}$ and $t_{1/2}$ by the same methods: A. C. Spivey, P. Charbonneau, T. Fekner, D. H. Hochmuth, A. Maddaford, C. Malardier-Jugroot, A. J. Redgrave, M. A. Whitehead, *J. Org. Chem.* **2001**, *66*, 7394.

12 A. Pal, M. Bérubé, D. G. Hall, *Angew. Chem., Int. Ed.* **2010**, *49*, 1492.

13 J. Yin, S. L. Buchwald, *J. Am. Chem. Soc.* **2000**, *122*, 12051.